Supporting Information

Gariépy et al. 10.1073/pnas.1113002109

SI Text

In Vitro Changes in Respiratory Activity. An in vitro preparation consisting of the isolated brainstem and a portion of the spinal cord was used to examine the role of central connections in the absence of sensory inputs (Fig. S1). Extracellular discharges were recorded from motoneurons in the glossopharyngeal motor nucleus (IX) or the rostral vagal motor nucleus (X) to monitor respiratory activity (at rest, 0.89 ± 0.30 Hz frequency; 54.5 ± 7.8 ms duration; Fig. 1 *B* and *B′* and Fig. S3). The mesencephalic locomotor region (MLR) was pharmacologically activated by locally injecting 2.5 mM D-glutamate (n = 48 injections, n = 7 preparations) and fictive locomotion, consisting of bilaterally alternating ventral root discharges, was elicited (Fig. S3*A*, *Center*). At the beginning of the fictive locomotor bout, a period of large and sustained tonic bursts replaced the short phasic bursts of respiratory activity. After this, respiration returned to a stable rhythmic pattern, but with a 91.4 ± 58.6% increase in frequency (0.89 ± 0.30 Hz in control to 1.57 ± 0.39 Hz; one-tailed paired t test; $P < 0.001$; n = 48) and a 58.2 ± 49.4% increase in area of the bursts (100 ± 14.4% in control to 157.8 ± 52.7%; one-tailed paired t test; $P < 0.001$; n = 48). The effects on the frequency lasted significantly longer than those on the burst area (154.6 ± 72.3 vs. 64.2 ± 35.3 s; two-tailed paired t test, $P < 0.001$; n = 48). In 23 cases, the changes in respiratory activity preceded locomotion, and in 25 cases, the respiratory changes followed the onset of locomotion. The delays ranged from −5.7 s to 1.6 s, with negative values indicating respiratory effects preceding locomotion. In a subset of four experiments, the paratrigeminal respiratory group (pTRG) was recorded in addition to the respiratory motoneurons, and similar respiratory changes were observed (Fig. S3*A*).

The intensity of the respiratory changes was correlated to the locomotor frequency (frequency, strong correlation; r = 0.72; linear fit; $P < 0.0001$; n = 48; area, weak correlation; r = 0.41; linear fit; $P < 0.01$; n = 48; Fig. S3*B*). In five additional experiments, the MLR was electrically stimulated (n = 163) at progressively increasing intensities (1–10 μA; 3 Hz; 2-ms pulse duration; 10 s) or frequencies (1–5 Hz; 5 μA; 2-ms pulse duration; 10 s; Fig. S3*C*). As previously shown in semi-intact lampreys (1), the locomotor frequency increased linearly with the stimulation intensity (average correlation coefficient r = 0.61 ± 0.13; linear fits; $P < 0.05$ for each preparation). In addition, the respiratory effects were correlated with the intensity of the MLR stimulation (average correlation coefficient for frequency r = 0.65 ± 0.17; linear fits; $P < 0.05$ for each preparation; area, r = 0.71 ± 0.14; linear fits; $P < 0.01$ for each preparation). These results show that, even in the absence of sensory feedback, the MLR induces respiratory effects in lampreys as previously seen in mammals (2–4).

We found that respiratory changes can occur in the absence of fictive locomotor activity from the ventral roots when the MLR was stimulated at weaker intensities (2 Hz; Fig. S3*C*). This suggests that the pathways increasing breathing can operate without actual movement. We also reproduced these results with local D-glutamate injections in the MLR (Fig. 1*D*). At such low stimulation strengths (20–86% of the intensity needed to induce locomotion), the respiratory frequency increased by 38.8 ± 24.8% (0.86 ± 0.15 Hz in control, 1.17 ± 0.20 Hz after stimulation; one-tailed paired t test, $P < 0.001$; n = 40) and the burst area by 11.0 ± 15.7% (100.0 ± 6.3% in control, 110.9 ± 16.9% after stimulation; Wilcoxon signed-rank test, $P < 0.001$; n = 40).

Resets of Respiratory Rhythm Following MLR Stimulation. To examine the physiological connections between the MLR and the respiratory central pattern generator, the former was stimulated with short trains of stimuli (100 Hz, n = 3 stimuli). We then determined whether there was a reset of the respiratory rhythm (n = 7 preparations, n = 2,053). When the stimulation was applied in the late phase of the respiratory cycle, a reset of the respiratory rhythm occurred immediately after the stimulus (Fig. S4 *A* and *B*, bracket 2), providing strong support for the presence of connections between the MLR and the respiratory central pattern generator. When the stimulation was delivered at the beginning of the cycle, the resetting effect occurred with a delay (Fig. S4 *A* and *B*, bracket 1). The respiratory frequency of the three respiratory bursts preceding the stimulation was significantly lower (1.06 ± 0.06 Hz) than that of the three respiratory bursts following the stimulation (1.25 ± 0.18 Hz; two-tailed t test, $P < 0.001$; n = 6,159 for both groups). Electrolytic lesions made at the end of these experiments confirmed that the stimulation site was located in the dorsal part of the MLR (Fig. S4*C*).

Retrograde Labeling of Population of MLR Cells Projecting to Respiratory Nuclei. Anatomical experiments were carried out by using retrograde tracers to reveal the population of MLR cells projecting to the respiratory nuclei. The cells presented in the main article were all labeled by using injections in the motor nuclei, but injections were also performed in the pTRG. Injections were made either in the pTRG on one side (n = 6 preparations), in the respiratory motoneuronal pools (n = 9 preparations), or in both the pTRG and the motoneuronal pools on the same side (n = 9 preparations; Fig. S5). Both motoneuronal pool and pTRG injections yielded retrogradely labeled cells in the ipsilateral and contralateral MLR (Fig. S5 *B* and *C*). The largest proportion of the labeled cells were found medially and dorsally within the isthmic periventricular cell layer, sometimes intermingled with the large neurons of the anterior rhombencephalic reticular nucleus. Very few cells were labeled more ventrolaterally in the isthmic tegmentum. Overall, numerous labeled cells were located in the area where electrolytic lesions were made as the MLR was physiologically identified (Fig. S4*C*). In double-labeling experiments, there were cells in the area containing both tracers (Fig. S5). The labeled cells in the MLR were counted in five preparations in which the pTRG and the motoneuronal pools were injected with different tracers. The counts were made every second section to avoid counting neurons twice. Therefore, the counts represent approximately half the population. Injections in the motoneuronal pools labeled on average 76 ± 35 neurons in the ipsilateral MLR and 16 ± 9 neurons in the contralateral MLR. Injections in the pTRG labeled 49 ± 41 neurons in the ipsilateral MLR and 35 ± 31 neurons in the contralateral MLR. Counts were also made in the nearby reticular nucleus, the anterior rhombencephalic reticular nucleus. No cells were labeled from the motoneuronal injections. pTRG injections labeled on average 8 ± 1 neurons in the ipsilateral MLR and 6 ± 4 contralaterally. On average, 6 ± 3 neurons were found double-labeled by the pTRG and motoneuronal pool injections when located on the same side, and 3 ± 1 neurons were double-labeled when the two injections were located on opposite sides. The experiments into which single MLR cells were injected with an intracellular dye revealed, on the contrary, that all the labeled MLR cells projected to the pTRGs and respiratory motoneurons on both sides (Fig. 3). The tracer injections in the pTRG could have destroyed some fibers that are descending to the motoneuronal pools or the injections may also miss some of

the axonal collaterals (Fig. S5). The neurons projecting to the pTRG and the respiratory motoneurons might thus be systematically underrepresented in the tracing experiments compared with single-cell injection experiments.

SI Materials and Methods

In Vivo Video Tracking. Experiments were conducted in vivo to evaluate the changes in respiratory frequency in relation to locomotion. Markers were used to track gill movements. The animals were anesthetized with tricaine methanesulfonate (MS 222, 100 mg/L). Six white dots (2 mm diameter, $n = 3$ ventrally, $n = 3$ dorsally) were tattooed on the skin of the gill region by using tattoo needles and white ink. The contractions of the gills during expiration were visible both ventrally and dorsally, such that respiratory movements could be tracked independently from the angle of the lamprey with respect to the camera. After the marking procedure, the animals were returned to their aquarium to recover from the procedure for at least 24 h. The animals were then transferred to a recording aquarium (98 × 35 cm) filled with 5 cm of water (approximately twice the height of lampreys). This allowed us to record swimming with reduced movements in the vertical plane, thus facilitating video tracking. The animals were allowed to acclimate for 2 to 4 h before data acquisition. The water temperature was kept between 8 °C and 10 °C. A video camera (GZ-HD3U; JVC) equipped with a wide-angle lens (0.42×) was placed below the aquarium (30 frames/s, 1,920 × 1,080 pixels). The recording sessions lasted several hours. The images were corrected for spatial distortion introduced by the wide angle.

Markers were manually pointed on the video images using homemade scripts in Matlab. The distance between any visible markers bilaterally placed on the gills provided a measure of respiratory movements. The low-frequency component of the measured distance signal was composed of various nonrespiratory signals such as movements across the aquarium and tilting. This component was removed by subtracting a moving average filtered version of the signal from the original signal at a frequency that was sufficiently low to leave any respiratory signal present (smooth function in Matlab; cutoff, 0.5 Hz). A moving average was then applied on the signal to remove high-frequency noise (smooth function in Matlab; cutoff, 6 Hz).

Locomotor movements were tracked by using markerless geometrical analysis of the body. The analysis relies on overlaying equidistant points on the body axis starting from the head down to the tail of the animal. The rostral extremity of the head was identified by the experimenter on every video frame. A set of pixels equidistant to the first point were calculated, thus forming a circle. The maximal contrast points along the circumference of that circle were found. These contrast points corresponded to the borders of the body. The mean angle between these two points with respect to the previous body point allowed calculating the position of the next body axis point. This analysis was repeated 10 times, providing a set of position vectors for 11 arbitrary equidistant segments of the body on every video frame. The angle between the point corresponding to segment i (P_i) and another point P_j with respect to a straight line defined by P_i and P_{i-1} provided a measure of local bending of the body between segments i and j. The angle signal was filtered using a band-pass filter based on moving averages similar to that for respiration (bandwidth, 0.5–6 Hz).

Resetting of Respiratory Rhythm. Whether electrical stimulation in the MLR induced phase shifts in the respiratory activity was tested by using an analysis similar to that of Morin and Viala (5). Phase shift was obtained by calculating a prediction of the respiratory period based on the mean period of the three preceding respiratory bursts (Pm; Fig. S4*B*). The shifted period (Ps) was obtained by measuring the period of the cycle modified by the stimulation. Dividing by Pm the difference between Ps and Pm provided a measure of how much the phase was shifted on a −1 to 0 scale (Fig. S4*B*, *y* axis). The phase of the stimulus was obtained by calculating L divided by Pm, where L is the latency between the stimulation and the preceding respiratory burst (Fig. S4*B*, *x* axis).

Histology and Axonal Tracing Experiments. In some preparations, electrolytic lesions were made in the MLR at the end of the electrophysiological experiments to confirm the exact position of the stimulation. The brain tissue was rapidly fixed by immersion in PBS solution (0.1 M, pH 7.4) containing 4% paraformaldehyde (Fisher Scientific) for 24 h at 4 °C. The tissue was then transferred in phosphate buffer (0.1 M, pH 7.4) containing 20% sucrose overnight at 4 °C. The next day, the tissue was quickly frozen at 50 °C in 2-methylbutane (Fisher Scientific) and cut transversally with a cryostat at 25 μm thickness. The transverse sections were mounted on ColorFrost Plus slides (Fisher Scientific), washed in PBS solution, stained with H&E, dehydrated in increasing concentrations of alcohol, cleared in xylene, and mounted with Entellan (EMD Chemicals).

In experiments in which patch-recorded cell projections were traced, the patch electrodes used contained 0.1% biocytin. The preparations were perfused with Ringer solution for 24 h after the experiment to allow biocytin to fill the injected neuron. The preparations were then fixed in paraformaldehyde, transferred in sucrose, and cut as described earlier. Biocytin was then revealed by using Alexa Fluor 488-conjugated streptavidin (Invitrogen) diluted (1:200) in PBS solution for 60 min at room temperature. The sections were then mounted with Vectashield/DAPI and observed and photographed with an Eclipse 600 microscope equipped with a DXM1200 video camera (Nikon).

1. Sirota MG, Di Prisco GV, Dubuc R (2000) Stimulation of the mesencephalic locomotor region elicits controlled swimming in semi-intact lampreys. *Eur J Neurosci* 12:4081–4092.
2. Eldridge FL, Millhorn DE, Waldrop TG (1981) Exercise hyperpnea and locomotion: Parallel activation from the hypothalamus. *Science* 211:844–846.
3. DiMarco AF, Romaniuk JR, Von Euler C, Yamamoto Y (1983) Immediate changes in ventilation and respiratory pattern associated with onset and cessation of locomotion in the cat. *J Physiol* 343:1–16.
4. Kawahara K, Nakazono Y, Yamauchi Y, Miyamoto Y (1989) Coupling between respiratory and locomotor rhythms during fictive locomotion in decerebrate cats. *Neurosci Lett* 103:326–330.
5. Morin D, Viala D (2002) Coordinations of locomotor and respiratory rhythms in vitro are critically dependent on hindlimb sensory inputs. *J Neurosci* 22:4756–4765.

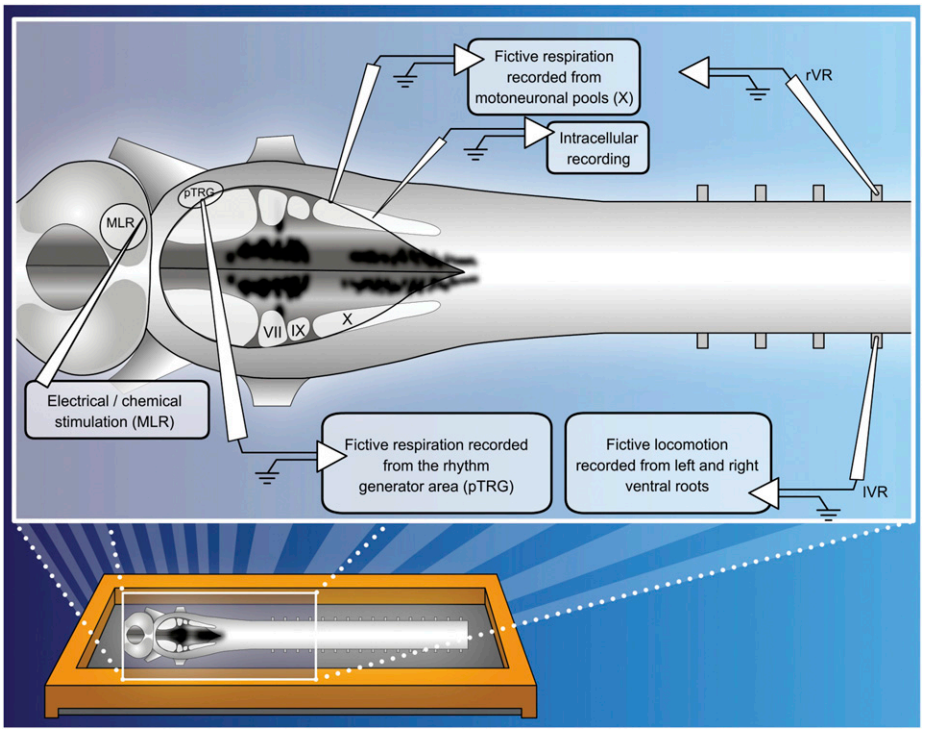

Fig. S1. Schematic representation of the experimental setup. Experiments were performed using chemical (D-glutamate 2.5 mM) or electrical stimulation (tungsten microelectrode) of the MLR. The respiratory activity was recorded using glass suction electrodes placed over the glossopharyngeal (IX) or the rostral vagal (X) motor nuclei. In some experiments, the pTRG was recorded in combination with respiratory motoneurons to monitor respiration. Locomotor activity was recorded by using glass suction electrodes placed on ventral roots on the right and left sides of the spinal cord ($_{R}$VR and $_{L}$VR, respectively). In some experiments, intracellular recordings of respiratory motoneurons in the IX or the X motor nucleus were carried out by using sharp microelectrodes. Injection micropipettes were placed in the pTRG on both sides to pressure-eject a mixture of 6-cyano-7-nitroquinoxaline-2,3-dione (CNQX) and (2R)-amino-5-phosphonovaleric acid (AP5). VII, facial motor nucleus.

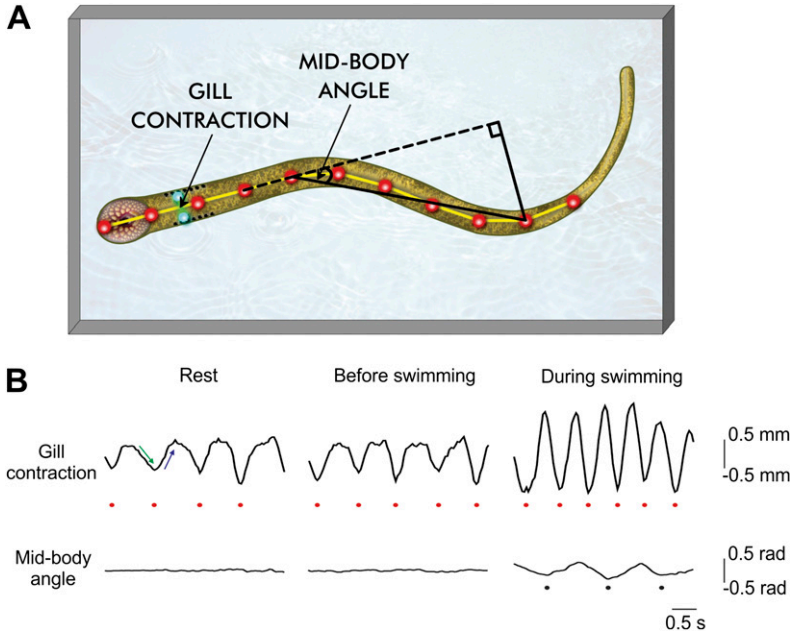

Fig. S2. In vivo respiratory increases associated with locomotion. (*A*) Schematic representation of the movement analysis procedure for respiratory and locomotor activities in freely moving adult lampreys. (*B*) Video tracking of respiratory and swimming movements at rest (*Left*), 6 s before swimming (*Center*), and during swimming (*Right*). Statistical analyses are provided in Fig. 1. Red dots indicate peaks of expiration, black dots indicate locomotor cycles, green arrow indicates expiration, and blue arrow indicates inspiration.

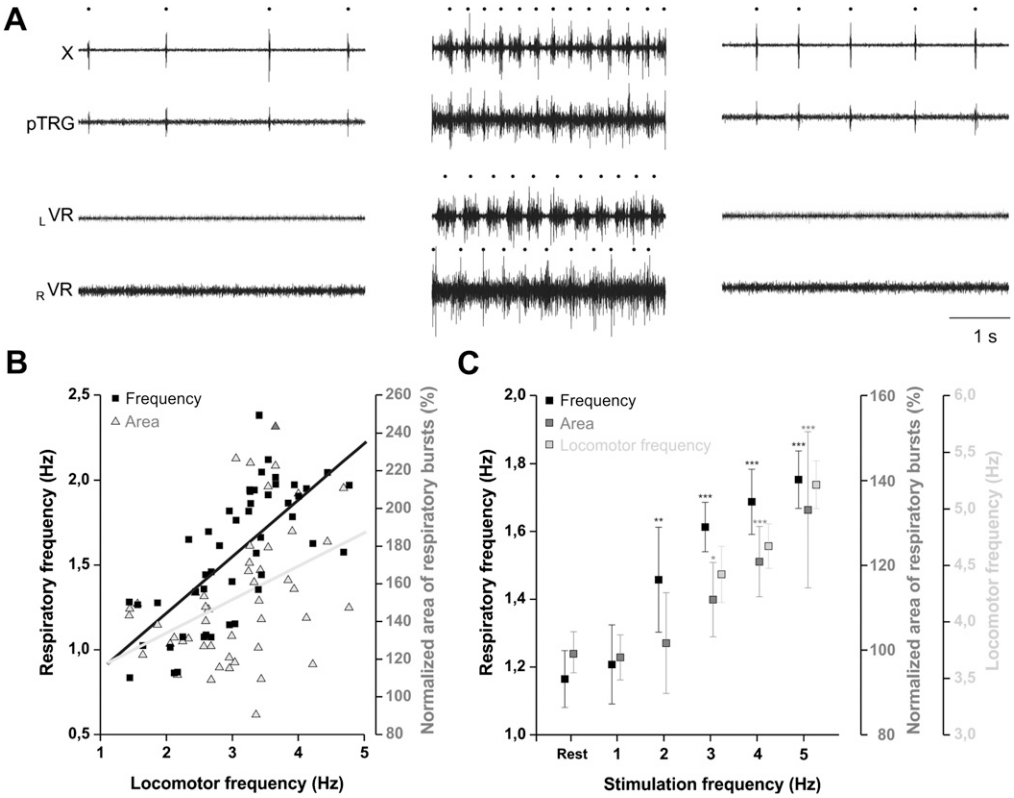

Fig. S3. Changes in respiratory activity associated with locomotion in an in vitro brainstem–spinal cord preparation. (*A*) Respiratory changes following D-glutamate (D-GLU, 2.5 mM) injection in the MLR. Neurographic recordings show the extracellular activity of the respiratory motoneurons (X), the pTRG, and left and right ventral roots of the spinal cord ($_{L}$VR and $_{R}$VR, respectively) before (*Left*), during (*Center*), and after (*Right*) fictive locomotion induced by chemical activation of the MLR. Dots indicate respiratory and locomotor bursts. (*B*) Graph illustrating the respiratory frequency and the normalized area of respiratory bursts vs. the locomotor frequency. Data were pooled from seven preparations (48 injections). (*C*) Graph illustrating the respiratory frequency, the normalized area of respiratory bursts, and the locomotor frequency vs. the MLR stimulation frequency. The data are illustrated for one preparation (*$P < 0.05$, **$P < 0.01$, and ***$P < 0.001$).

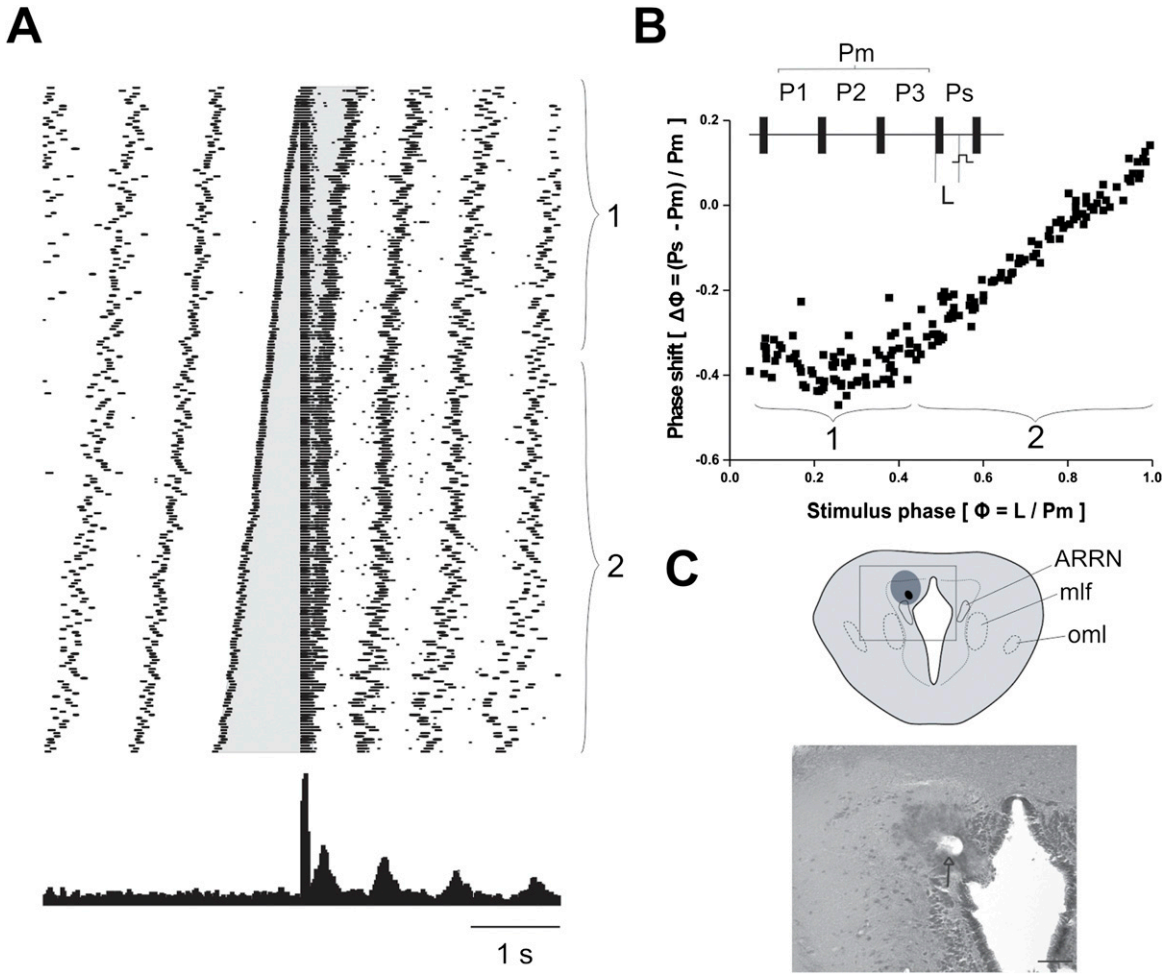

Fig. S4. Resetting of the respiratory rhythm by short trains of electrical stimulation of the MLR. (*A*) Raster representation of extracellular activity recorded from the vagal motor nucleus aligned on the onset of MLR stimulation (vertical line, middle). Stimulation (trains of three stimuli at 100 Hz) was performed at different phases of the respiratory cycle (bracket 1, early during the cycle; bracket 2, late in the cycle). The gray area shows the respiratory cycle during which the stimulation is delivered. The histogram below shows the summation of the raster points (bin width, 20 ms). (*B*) Plot of the phase shift vs. stimulus phase. Note that a linear relationship between phase shift and stimulus phase is only present for Φ values greater than 0.4. (*C*) A typical MLR stimulation site identified by an electrolytic lesion. *Top*: Schematic illustration of a transverse section of the brainstem at the level of the isthmus. *Bottom*: Photomicrograph illustrating the electrolytic lesion, which is located in the MLR. (Scale bar: 50 μm.) ARRN, anterior rhombencephalic reticular nucleus; mlf, medial longitudinal fasciculus; oml, lateral octavomesencephalic tract (***$P < 0.001$).

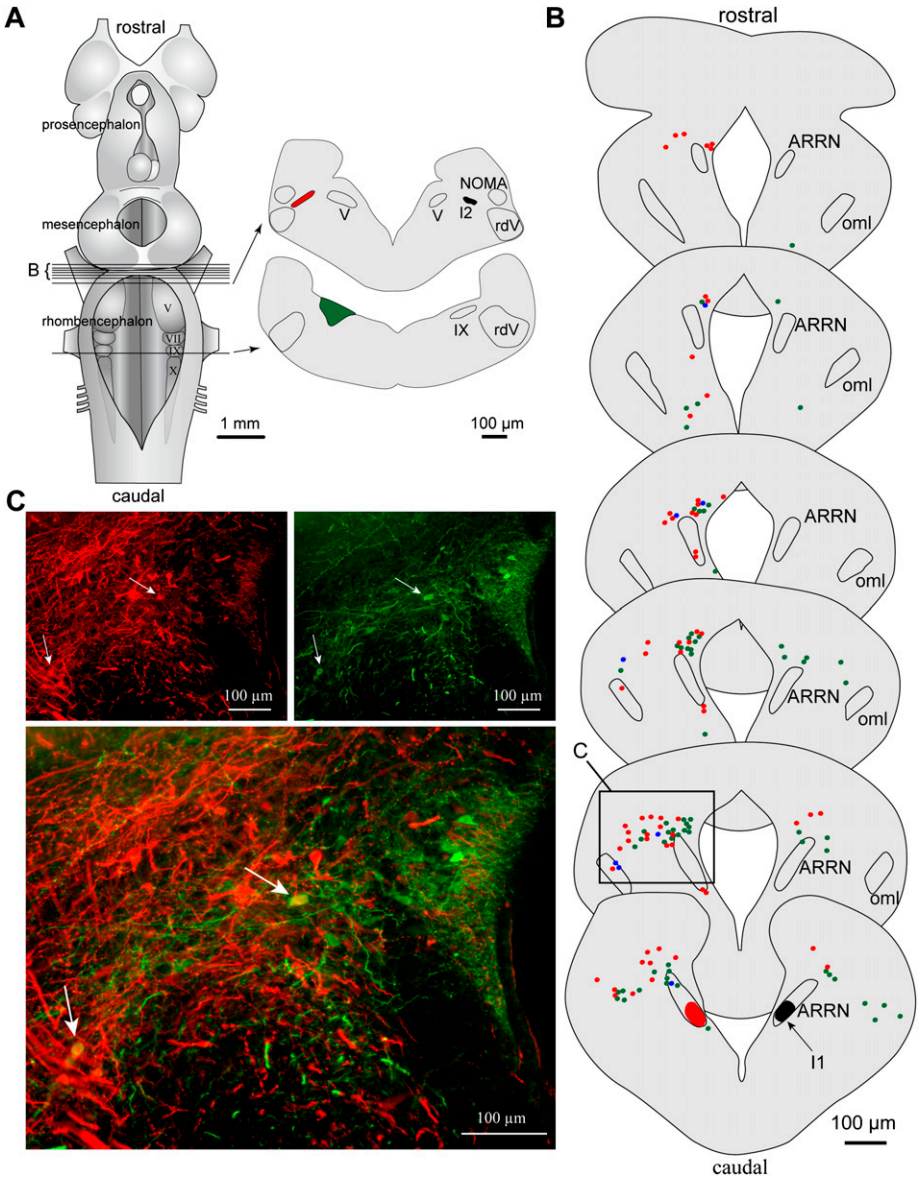

Fig. S5. Distribution of neurons in the MLR projecting to the pTRG and/or to respiratory motoneurons. (*A*) Schematic dorsal view of the lamprey brain indicating the levels of the transverse sections illustrated in *B*. *Right*: Schematized transverse sections at the levels of the tracer injections in the pTRG (red) and the respiratory motoneurons (green). (*B*) Transverse sections in the MLR showing retrogradely labeled neurons from the two injection sites. A section was skipped between each illustrated one to avoid including some neurons twice. Each dot represents a labeled neuron. Double-labeled neurons are represented by blue dots. (*C*) Photomicrographs of the boxed area in *B* with neurons labeled from the pTRG (red) and from the vagal motor nucleus (green). The arrows indicate double-labeled neurons, which appear in yellow on the superimposed images. ARRN, anterior rhombencephalic reticular nucleus; NOMA, anterior octavomotor nucleus; oml, lateral octavomesencephalic tract; rdV, descending trigeminal root; V, trigeminal nucleus; VII, facial motor nucleus; IX, glossopharyngeal motor nucleus; X, vagal motor nucleus. I1 and I2 are two large reticulospinal cells used as anatomical landmarks.

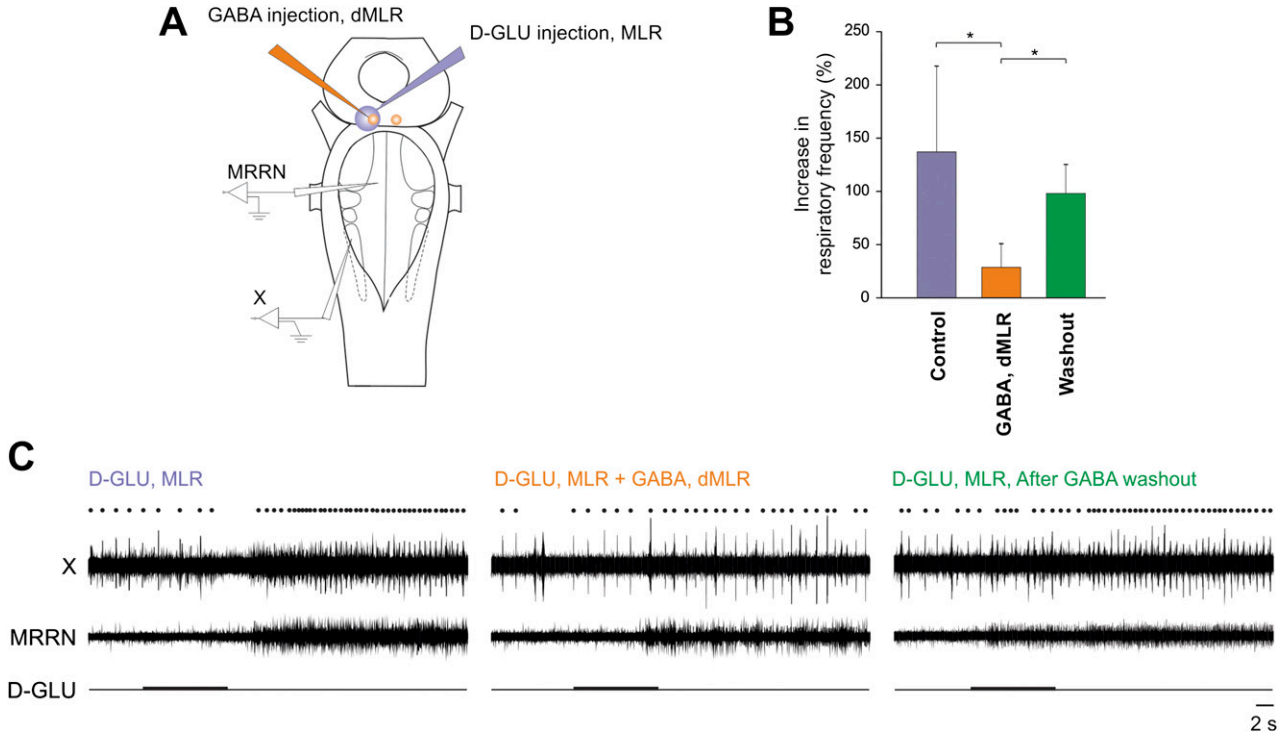

Fig. S6. Effect of a GABA injection in the dorsal part of the MLR on the MLR-induced respiratory increases. (*A*) Schematic dorsal view of the in vitro brainstem preparation indicating the injection sites for D-glutamate (D-GLU, 2.5 mM), GABA (1 mM), and the recording sites [middle rhombencephalic reticular nucleus (MRRN) and X]. (*B*) Analysis of the increases in respiratory frequency following D-glutamate injections in the MLR in the control condition, after GABA injection bilaterally in the dorsal part of the MLR, and after washout. D-glutamate injections were performed every 20 min. First, a control injection was made. It was followed by a D-glutamate injection immediately after injecting GABA (<1 min). After 20 min of washout, a third D-glutamate injection was made. These experiments were performed on five preparations. The GABA injection markedly reduced the increase in respiratory frequency induced by the D-glutamate injection (137.0 ± 80.6% in control, 28.7 ± 22.2% after GABA; ANOVA on ranks; $n = 5$ injections; $P < 0.05$). After washout, the effect recovered (98.0 ± 27.2%; ANOVA on ranks; $n = 5$ injections; $P < 0.05$ for difference with effect, $P > 0.05$ for difference with control). (*C*) Raw traces of the MLR-induced respiratory effects (*$P < 0.05$). D-GLU, D-glutamate; X, vagal motor nucleus; dMLR, dorsal part of the MLR. Dots indicate expiratory activity.